Electrochemical Activation of Metal Hydride Alloy by Inclusion of Nickel and Palladium Nanoparticles

M.A. Rivera[1,*], S.A. Gamboa[2] and P.J. Sebastian[2,†]

[1]Universidad Politécnica del Estado de Guerrero, Carretera Taxco-Iguala, Ejido de Arroyo s/n, CP. 40290, Taxco Guerrero México
[2]Departamento de Materiales Solares, Centro de Investigación en Energía, Universidad Nacional Autónoma de México, Xochicalco S/N, Centro, 62580, Temixco, Morelos, México.

Abstract: *Nickel and palladium nanoparticles were obtained by colloidal dispersion. Chemical reduction was used to obtain good quality nanoparticles showing electrocatalytic characteristics for improving the electrochemical hydrogen content in typical metal hydride at the initial stage of absorption process. The particle size and distribution of the colloidal nanoparticles were calculated by analyzing TEM images. The colloidal nanoparticles obtained were impregnated onto $LaNi_{5-x}M_x$ type metal hydride alloy via catalytic dipping. The impregnated metal hydride alloy was characterized by SEM, AFM and EDS to obtain quasi-quantitative measurements of the position and concentration of the agglomerated colloidal nanoparticles forming nano-clusters onto de surface of the metal hydride alloy. Electrochemical characterization showed the enhancement of absorbed hydrogen content in the metal hydride due to the presence of agglomerated nanoparticles and the localized catalytic activity of Pd more than that of Ni nano-clusters.*

1. INTRODUCTION

In recent years, nanoparticles are subjected to intensive research and development because of their fascinating properties and potential applications. For example, magnetic and spectroscopic properties of quantum sized semiconductors, synthesis and characterization of polymers and stabilizers for the binding of metal nanoparticles, nanoparticle spectroscopic investigations in the gas phase studies of metals and ceramics etc. [1,4]. Such nanoparticles having a diameter of 1-10 nm are creating a new category of materials, which behave differently from its conventional macroscopic form. This category can be called "ensemble of atoms" or "molecule," [5,6].

Recent studies have shown that the size of the nanoparticle promotes chemical reactivity [7], with increased active surface area relative to volume. This property is very important in the field of catalysis. It is also very important to protect the nanoparticles to prevent them from regrouping and form large structures [8]. The introduction of nanomaterials in energy storage systems can have multiple impacts: improving the life cycle, improve stability, easy to produce and handle, high electronic conductivity, increased power density etc.

The materials capable of electrochemical hydrogen storage are needed for use as negative electrode in various applications of mobile electronics and electric vehicles. In the past decades, many metal hydride alloys were investigated and have been used successfully in commercial batteries [9, 11]. To improve the energy density of batteries and electrochemical systems, the search for new materials for hydrogen storage has been carried out on spatially continuous nano-sized materials. These materials can be an alternative to produce hydrogen storage electrodes [12-13]. In recent years, a number of nanotubes [14-18] and alloy nanoparticles [19-21] have shown the hydrogen storage capabilities.

The case of metal hydrides is important, because it can be applied to hydrogen storage systems. Nickel-metal hydride (Ni-MH) batteries have a voltage, rate capability, overcharge protection and self-discharge comparable to that of nickel-cadmium (Ni-Cd) batteries [22]. The metal-hydride batteries not only provide increased energy density (the energy density of the Ni-MH cell is about 75% higher that of Ni-Cd cells), but are also environmentally benign

Figure 1a. TEM micrograph for the colloidal Pd nanoparticles
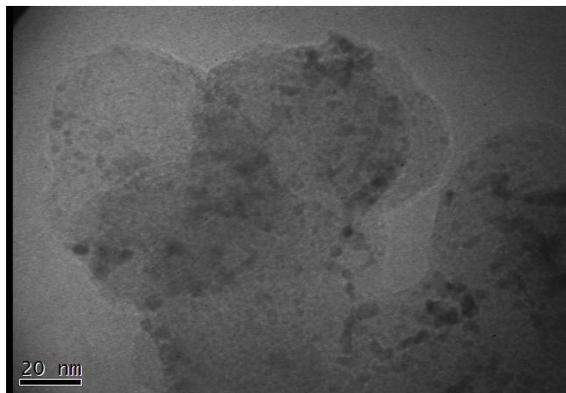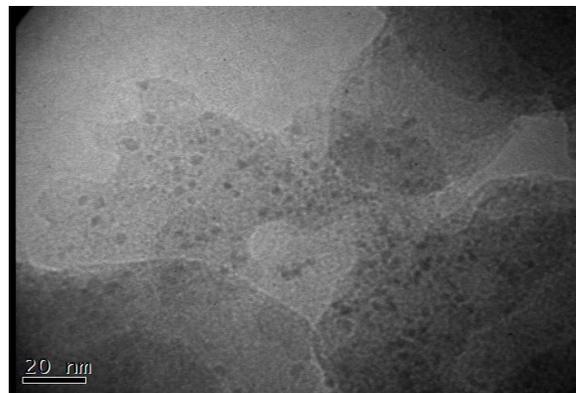

Figure 2a. TEM micrograph for the colloidal nanoparticles of Ni

Figure 1b. Histogram of the particle size distribution for the Pd nanoparticles
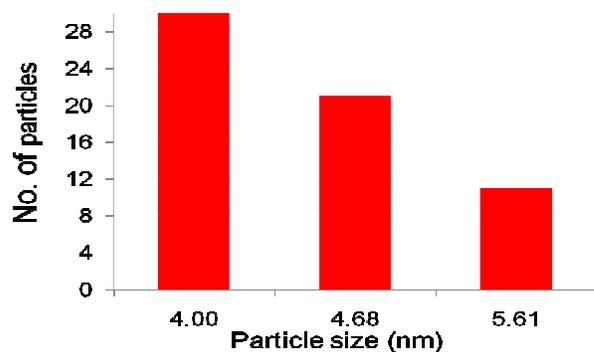

Figure 2b. Histogram of the particle size distribution for the Ni nanoparticles

with less severe disposal problems. However, the Ni-MH batteries lose about 30% of their capacity by self-discharge in 1 month of storage, which is slightly higher than that of Ni-Cd batteries.

A common strategy employed to improve the performance of the negative electrode in Ni-MH batteries is to microencapsulate the metal hydride alloy particles with various kinds of electroless coating such as Cu, Ni-P, Ni-B, Pd and Ni [23-26]. In this study, we prepared Pd-Ni and Ni as nanostructure materials to be incorporated into the negative electrode.

2. EXPERIMENTAL DETAILS

The multicomponent material $(La_{0.55}Ce_{0.3}Nd_{0.11}Pr_{0.04})$ $(Co_{0.14}Al_{0.08}Mn_{0.06}Ni_{0.71})_{5.02}$ was used in this work as the active metal hydride alloy. It was obtained from Rhodia Inc. and the experimental preparation details were discussed elsewhere [27].

2.1. Preparation of Pd and Ni based nanoparticles

Colloidal Pd nanoparticles were prepared by reduction of Pd-salt at inert atmosphere. $PdCl_2$ solution was prepared in 25 ml methanol at 0.033 mmol concentration using $PdCl_2$ chemical reagent (99.9 % purity, Alfa Aesar). After the solution was prepared, 25 ml of poly(N-vynil-2-pyrrolidone) was added to the solution to maintain the nanoparticles in colloidal form. 50 ml methanol was added to complete a 100 ml full volume. The solution was de-aerated by

bubbling argon for 1 hr at 50 °C under stirring conditions; then 3 ml/0.022M $NaBH_4$ aqueous solution was added to the solution, the $NaBH_4$ aqueous solution was maintained at 25°C. Pd nanoparticles in methanol complex were formed by this method. The nanostructural characteristics of the Pd particles prepared by this method have been discussed in a previous report [28]. Methanol solutions of $NiSO_4 \cdot 6H_2O$ (99.9 % Sigma, 0.033 mmol in 25 ml of methanol) were prepared in the similar way.

2.2. Impregnation procedure

Metal hydride alloy powder based on $(La_{0.55}Ce_{0.3}Nd_{0.11}Pr_{0.04})$ $(Co_{0.14}Al_{0.08}Mn_{0.06}Ni_{0.71})_{5.02}$ was impregnated with Pd and Ni nanoparticles. The experimental impregnation procedure details have been discussed elsewhere [29].

2.3. Metal hydride electrode preparation

INCO T-210 nickel powder was added as additive at 1:1 weight ratio to the Pd or Ni nanoparticle incorporated metal hydride alloy. The particle size of the additive was 1±0.5 mm. Pd free nickel foam was used as substrate and 500 MPa-cm^{-2} mechanical pressure was applied to form the electrode, obtaining a laminar electrode as discussed elsewhere [29].

The electrochemical characterization was performed in a three compartment open cell with 6M KOH aqueous solution as electro-

Electrochemical Activation of Metal Hydride Alloy by Inclusion of Nickel and Palladium Nanoparticles
/ J. New Mat. Electrochem. Systems

33

lyte. The metal hydride electrode was used as the working electrode, a Hg/HgO electrode as reference electrode and a (Ni(OH)$_2$/NiOOH) electrode as counterelectrode. A solartron potentiostat/galvanostat model SI 1287 with impedance analyzer model SI 1260 and corrware software attached to a computer interface was used to perform and record the experiments.

3. RESULTS AND DISCUSSION

3.1. Transmission Electron Microscopy Characterization

Figure 1 (a) shows the transmission electron micrograph (Philips Tecnai 200 TEM operated at 200 keV) of palladium nanoparticles synthesized using the colloidal dispersion technique. Figure 1 (b) shows the histogram of the size distribution of 60 nanoparticles quantified, which have an average size of 5.088 nm, with a standard deviation of ± 1.338.

Figure 2 (a) shows the transmission electron micrograph of nickel nanoparticles synthesized using the same technique and figure 2 (b) shows the histogram of the size distribution of 62 nanoparticles quantified, which has an average size of 4.516 nm, with a standard deviation ± 0.596. As shown in TEM characterization technique, one can appreciate the existence of Pd nanoparticles of the order of 5.088 nm and Ni particles the order of 4.516 nm.

3.2. Results of Energy Dispersive Spectroscopy Analysis

The nanoparticles of Pd and Ni obtained were impregnated on the surface of the particles of the metal hydride. Using the energy dispersive spectroscopy technique we quantified the weight percentage and atomic percentage of elements present in the samples. Table 1 shows the elements present and the atomic percentage of the sample of metal hydride and metal hydride impregnated with Pd and Ni nanoparticles. It is also shown the elements that form the metal hydride and for the sample impregnated with nanoparticles of Pd. It is seen in the table (shown in dark) the increasing content of Pd from 0 to 1.22 atm. %, so does the sample impregnated with nanoparticles of Ni, from 53.45 to 59.89 atm.%.
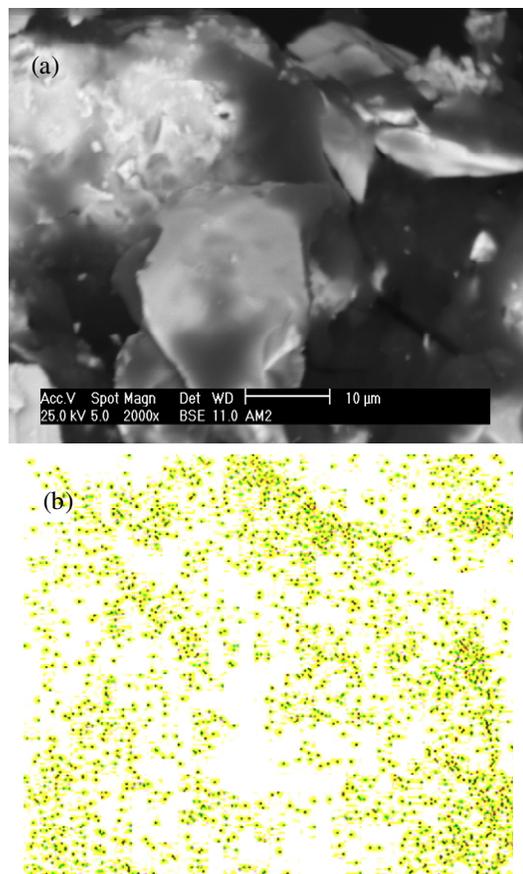

Figure 3. (a) The SEM micrograph for the AB$_5$ type metal hydride impregnated with Pd nanoparticles; (b) The elemental mapping for Pd distributed on the metal hydride particles

3.3. Results of Scanning Electron Microscopy Analysis and Elemental Mapping

Figure 3 (a) shows the image obtained by SEM technique for

Table 1. Energy dispersive spectroscopy analysis results showing the elements present on the surface of Pd and Ni nanoparticle impregnated metal hydride.

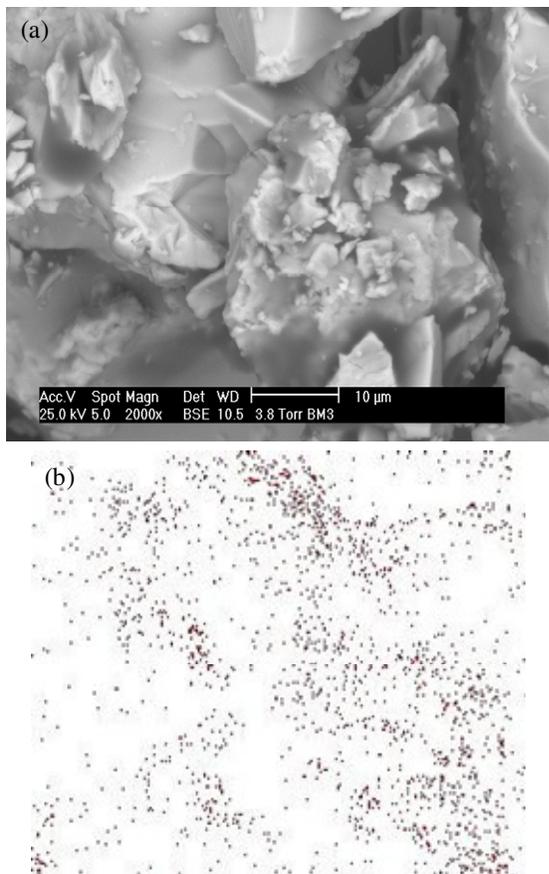| Metal Hydride (MH)		MH-Nanoparticles of Pd		MH-Nanoparticles of Ni	
Element	Atomic %	Element	Atomic %	Element	Atomic %
AlK	14.76	AlK	7.34	AlK	8.30
PdL	0.00	PdL	1.22	PdL	0.00
LaL	8.69	LaL	8.81	LaL	8.57
CeL	5.12	CeL	5.13	CeL	5.18
PrL	0.86	PrL	0.94	PrL	0.92
NdL	2.20	NdL	1.98	NdL	2.14
MnK	4.30	MnK	4.70	MnK	4.47
CoK	10.63	CoK	10.89	CoK	10.52
NiK	53.45	NiK	53.45	NiK	59.89
Total	100.00	Total	100.00	Total	100.00

Figure 4. (a) The SEM micrograph for the AB$_5$ type metal hydride impregnated with Ni nanoparticles; (b) The elemental mapping for Ni distributed on the metal hydride particles
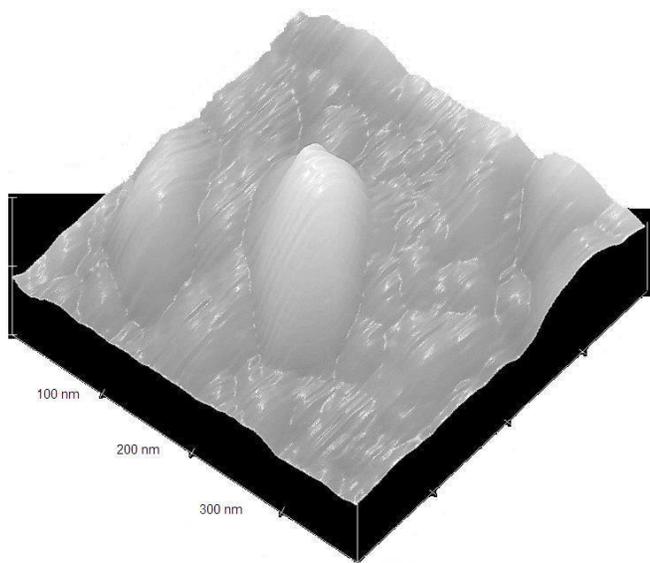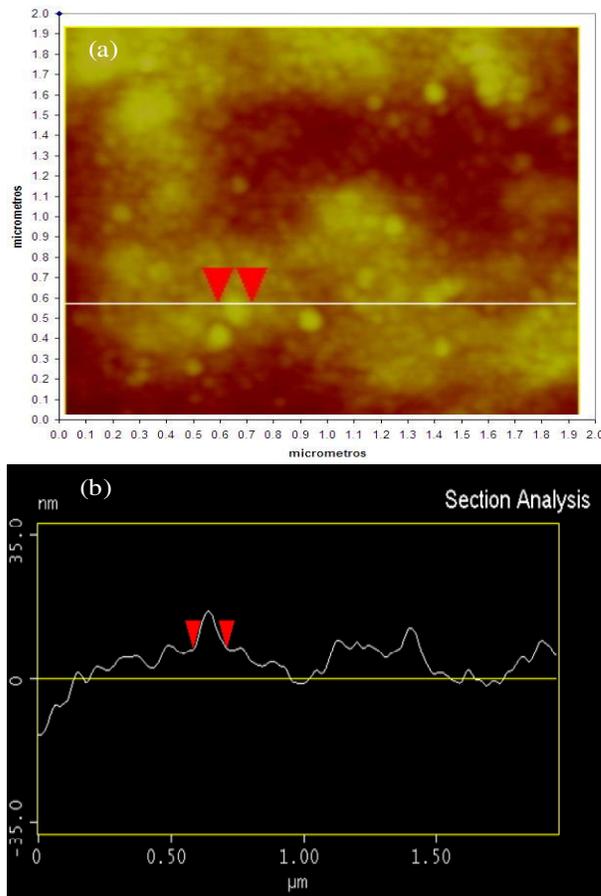

Figure 6. (a) The AFM micrograph of the metal hydride surface analyzed for Pd; (b) as a function of longitude and height

Figure 5. The morphology of the Pd nanoparticles supported on the metal hydride surface

metal hydride impregnated with palladium nanoparticles with a nominal composition of 1:1, at 10 mm. In this image one can observe only the morphology of the particles of unidentified hydride impregnated nanoparticles.

Figure 3 (b) shows the elemental mapping performed on metal hydride particles impregnated with palladium nanoparticles, the black dots represent the palladium, heterogeneously distributed on the surface of the sample, confirming the presence of nanoparticles on the surface of the metal hydride.

Figure 4 (a) shows the image obtained by SEM technique for metal hydride nickel nanoparticles impregnated with nominal composition of 1:1 at 10 mm. In this image one can observe only morphology of unidentified impregnated nanoparticles. Figure 4 (b) shows the elemental mapping performed on metal hydride particles impregnated with nickel nanoparticles, the black dots represent the nickel distributed heterogeneously on the sample surface, confirming the presence of nanoparticles on the surface of the metal hydride.

3.4. Results of Atomic Force Microscopy (AFM) Analysis

Figure 5 shows the image obtained using the AFM technique for the topography of the Pd nanoparticles supported on metal hydride

Electrochemical Activation of Metal Hydride Alloy by Inclusion of Nickel and Palladium Nanoparticles
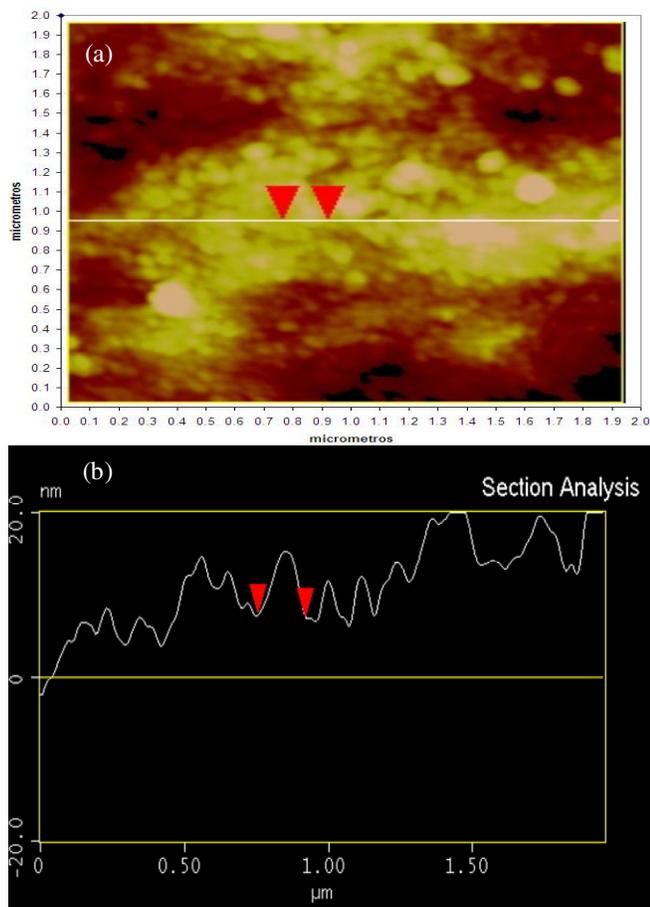*/ J. New Mat. Electrochem. Systems*

35

Figure 7. (a) The AFM micrograph of the metal hydride surface analyzed for Ni; (b) as a function of longitude and height

surface; the image confirms that colloidal nanoparticles adhere to the surface in the form of "cluster".

Figure 6 (a) shows the image of the AFM micrograph of Pd nanoparticles supported on a metal hydride surface. As shown in the picture there is a color change of light and dark, this change in the color identifies the phases present. The dark phase corresponds to the metal hydride and the light phase corresponds to the phase of the Pd nanoparticle cluster. Figure 6 (b) shows the image of the micrograph, which shows the distance of the cantilever and the height of the Pd clusters in micrometers. The cluster indicated by the arrows is 0.2 mm (200 nm) wide and 17.5 m high, thick white line indicates the relative area of the metal hydride.

Figure 7 (a) shows the image of the AFM micrograph of Ni nanoparticles supported on a metal hydride surface. As seen in the picture the color change of light and dark identifies the phases present. The dark phase corresponds to the metal hydride and the light phase corresponds to the cluster of nanoparticles of Ni. Figure 7 (b) shows the image of the micrograph, which displays the distance of the cantilever and the height of the Ni cluster in micrometers, the cluster indicated by the arrows is 0.14516 m m (145.16 nm) wide and 17.5 nm high, thick white line indicates the relative area of the metal hydride.
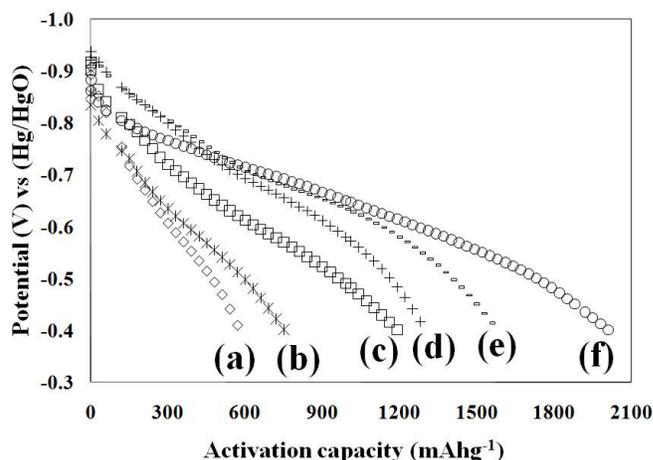

Figure 8. The comparison of the 1st and 2nd discharge cycles of the metal hydride electrode and that impregnated with Pd and Ni nanoparticles; (a) cycle 1 MH, (b) cycle 1 MH-Ni, (c) cycle 1 MH-Pd, (d) cycle 2 MH, (e) cycle 2 MH-Ni, (f) cycle 2 MH-Pd.
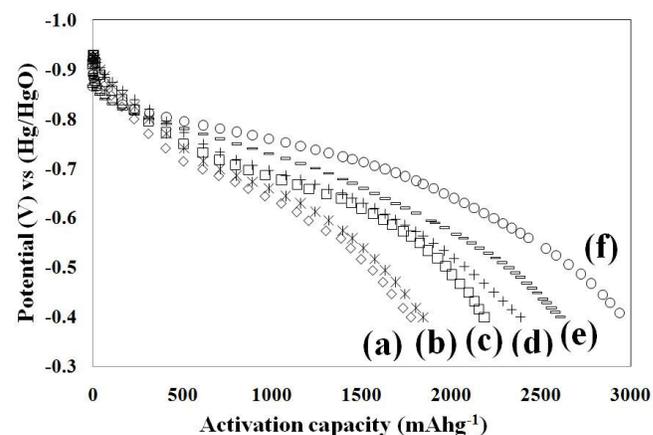

Figure 9. The comparison of the 1st and 2nd discharge cycles of the metal hydride electrode and that impregnated with Pd and Ni nanoparticles; (a) cycle 3 MH, (b) cycle 3 MH-Ni, (c) cycle 3 MH-Pd, (d) cycle 4 MH, (e) cycle 4 MH-Ni, (f) cycle 4 MH-Pd.

3.5. Activation

Figure 8 shows the first two discharge cycles corresponding to the initial state of the absorbing hydrogen in metal hydride electrode and metal hydride electrodes impregnated with Pd and Ni nanoparticles. The discharge current for the three electrodes was 50 mAg^{-1}.

Figure 9 represents the third and fourth discharge cycles for the electrodes. It can be observed that the activation capability of metal hydride electrode impregnated with palladium, in the first four cycles, is beyond the capacity of activation for the metal hydride electrode base metal and impregnated nickel. In the subsequent cycles the activation capacity of the electrode impregnated with palladium remains slightly high compared to the electrode impregnated with nickel and double for the base metal hydride electrode. The presence of palladium nanoparticles contribute mainly to the

catalytic activity of the surface hydride, facilitating the charge transfer process for the reduction of hydrogen ion, although the amount of hydrogen absorbed in palladium nanoparticles cannot be quantified by the method of loading / unloading,. The amount is very small, so that the contribution of this storage is negligible, but these results provide evidence that the incorporation of nanoparticles of palladium facilitates the absorption process in the state and the activation of the metal hydride quickly.

4. CONCLUSIONS

We achieved the synthesis of nanoparticles based on palladium-nickel and nickel by colloidal dispersion chemical technique with an average particle distribution of 5.088 nm for Pd and 4.516 nm for Ni. The nanoparticles showed catalytic properties that favored the absorption of hydrogen in the metal hydride. The impregnation technique used was appropriate, as it confirmed the presence of nanoparticles on the surface of the metal hydride in the form of cluster. The absorption properties of hydrogen in metal hydride were the basis of the impregnation technique of nanoparticles on the active material. The activation properties of the metal hydride are favored mainly by palladium nanoparticles, compared to nickel and the base metal hydride.

5. ACKNOWLEDGEMENTS

REFERENCES

[1] J.H. Fendler, "Nanoparticles and Nanostructured Films: Preparation, Characterization and Applications", ed., Wiley-VCH, Weinhein/New York, USA, 1998.

[2] G. Schmid, Clusters and Colloids: From Theory to Application, VCH, Weinheim, Germany, 1994.

[3] P.V. Kamat, Chem. Rev., 93, 267 (1993).

[4] B. C. Gates, Chem. Rev., 95, 511 (1995).

[5] R.W.J. Scott, M.J. MacLachlan, G.A. Ozin, Curr. Opin. Solid State Mat. Sci., 4, 113 (1999).

[6] R. Schuster, V. Kirchner, P. Allongue, G. Ertl, Science, 289, 98 (2000).

[7] T. Delwing, G. Rupprechter, H. Unterhalt, H.J. Freund, Phys. Rev. Lett., 85, 776 (2000).

[8] M. Brust, M. Walker, D. Bethell, D.J. Schiffrin, R. Whyman, J. Chem. Soc.: Chem. Commun., 801, (1994).

[9] U. Köhler, J. Kümper, M.J. Ullrich, J. Power Sources, 105, 139 (2002).

[10] Y. Liaw, X.G. Yang, Solid State Ionics, 152, 217 (2002).

[11] X.P. Gao, Y. Wang, Z.W. Lu, W.K. Hu, F. Wu, D.Y. Song, P.W. Shen, Chem. Mater., 16, 2515 (2004).

[12] X.P. Gao, Z.W. Lu, Y. Wang, F. Wu, D.Y. Song, P.W. Shen, Electrochem. Solid State Lett., 7, A102 (2004).

[13] Xuedong Wei, Rui Tang, Yongning Liu, Peng Zhang, GuangYu, Jiewu Zhu, International Journal of Hydrogen Energy, 31, 1365 (2006).

[14] J. Chem, S.L. Li, Z.L. Tao, Y.T. Shen, C.X. Cui, J. Am. Chem

Soc., 125, 5284 (2003).

[15] Xianjuan Fu, Haiyan Zhang, Yiming Chen, Shunhau Li, Shuangping Yi, Chun Zhou, Minghua Li, Yanjuna Zhu, Jin Chen, Physica E, 25, 414 (2005).

[16] Shuangping Yi, Haiyan Zhang, Lei Pei, Yanjuan Zhu, Xiaoling Chen, Xinming Xue, Journal of Alloys and Compounds, 420, 312 (2006).

[17] Z.W. Lu, S.M. Yao, G.R. Li, J.Q. Qu, X.P. Gao, Journal of Alloys and Compounds, 463, 378 (2008).

[18] A. Reyhani, S.Z. Mortazavi, A.Z. Moshfegha, A. Nozad Golikand, M. Amiri, Journal of Power Sources, 188, 404 (2009).

[19] R.G. Gao, J.P. Tu, X.L. Wang, X.B. Zhang, C.P. Chen, Journal of alloys and Compounds, 356-357, 649 (2003).

[20] Huaiyu Shao, Yunao Wang, Hairuo Xu, Xingguo Li, Journal of Solid State Chemistry, 178, 2211 (2005).

[21] S.R. Chung, K.W. Wang, M.H. Teng, T.P. Perng, International Journal of hydrogen energy, 34, 1383 (2009).

[22] M.V.C.Sastri, B.Viswanathan, S.Srinivasa Murthy, Metal Hydrides- Fundamentals and Applications, Narosa Publishing House, New Delhi, India, 1998.

[23] C. Iwakura, Y. Kajiya, H. Yoneyama, T. Sakai, K. Oguro, H. Ishikawa, J. Electrochem Soc., 136, 1351 (1989).

[24] M. Raju, M.V. Ananth, L. Vijayaraghavan, Journal of Alloys and Compounds, 475, 664 (2009).

[25] Xianjiu Zhao, Qian Li, Kuochih Chou, Hui Liu, Genwen Lin, Journal of Alloys and Compounds, 473, 428 (2009).

[26] Yanzhi Wang, Minshou Zhao, Limin Wang, International Journal of hydrogen energy, 34, 2646 (2009).

[27] S.A. Gamboa, P.J. Sebastian, Int. J. Hydrogen Energy, 26, 117 (2001).

[28] U. Pal, J.F. Sánchez-Ramírez, S.A. Gamboa, P.J. Sebastian, R. Pérez, Physic Status Solid (c), 0, 2944 (2003).

[29] M.A. Rivera, U. Pal, Xianyou Wang, J.G. Gonzalez-Rodriguez, S.A. Gamboa, Journal of Power Sources, 155, 470 (2006).